

Energy-Based Generative Cooperative Saliency Prediction

Jing Zhang¹ Jianwen Xie² Zilong Zheng³ Nick Barnes¹

¹ Australian National University ² Baidu Research ³ University of California, Los Angeles
zjnwpu@gmail.com, {jianwen, zilongzheng0318}@ucla.edu, nick.barnes@anu.edu.au

Abstract

Conventional saliency prediction models typically learn a deterministic mapping from images to the corresponding ground truth saliency maps. In this paper, we study the saliency prediction problem from the perspective of generative models by learning a conditional probability distribution over saliency maps given an image, and treating the prediction as a sampling process. Specifically, we propose a generative cooperative saliency prediction framework based on the generative cooperative networks, where a conditional latent variable model and a conditional energy-based model are jointly trained to predict saliency in a cooperative manner. We call our model the SalCoopNets. The latent variable model serves as a fast but coarse predictor to efficiently produce an initial prediction, which is then refined by the iterative Langevin revision of the energy-based model that serves as a fine predictor. Such a coarse-to-fine cooperative saliency prediction strategy offers the best of both worlds. Moreover, we generalize our framework to the scenario of weakly supervised saliency prediction, where saliency annotation of training images is partially observed, by proposing a cooperative learning while recovering strategy. Lastly, we show that the learned energy function can serve as a refinement module that can refine the results of other pre-trained saliency prediction models. Experimental results show that our generative model can achieve state-of-the-art performance. Our code is publicly available at: <https://github.com/JingZhang617/SalCoopNets>.

1. Introduction

Salient object detection has addressed a large amount of interest in the computer vision community over the recent years for its close relation to human’s visual perception and effectiveness of representing the entire scene. The *salient region*, referred as the visually distinctive scene region that can be perceived by human effortlessly and rapidly before further processing, is commonly treated as a pixel-wise binary output of a deterministic prediction model in most re-

cent works [45, 33, 46, 42, 39, 24, 43].

Despite the success of achieving a highly accurate saliency map in prior work, such processes commonly have limited diversity in their generated results because of their deterministic nature, in contrast to human vision, *i.e.* the process of selecting salient regions is subjective for each observer [14] and will be affected by a set of factors, including biological (*e.g.* contrast, sensitivity), and contextual (*e.g.* task, experience, interests), *etc.*

Generative models, on the other hand, have demonstrated their ability to produce diverse plausible outputs given the same input [67, 20]. The problem is typically modeled in a conditional generation setting and the goal is to generate diverse outputs that match the condition in context and differ in style. In this work, we fit the saliency detection task into this framework, where the observed images are input conditions, and aim to generate diverse possible saliency maps. Rather than implicitly modeling the distribution of outputs using GAN-based frameworks [8, 13], we additionally propose to model the conditional distribution of saliency maps *explicitly* in an energy-based framework, which is well-known for its flexibility and effectiveness in distribution parameterization [47, 48, 7, 31]. Typically, the energy-based model (EBM) learns an energy function by maximum likelihood estimation (MLE) and generates outputs via an iterative sampling process using Markov Chain Monte Carlo (MCMC) given the updated energy function. However, this framework commonly suffers from difficulties in modeling high-dimensional data, and from the computational expensiveness of MCMC.

Inspired by prior success of cooperative training in unconditional image generation [47], in this work, we bring the best of both worlds, saliency prediction models and EBMs, into one framework and propose a *conditional cooperative saliency prediction network* for modeling the visual saliency distribution and generating diverse yet meaningful saliency maps. The proposed model is called the SalCoopNets. Specifically, the model consists of a conditional energy-based model (EBM) whose energy function is parameterized by a bottom-top neural network, and a conditional latent variable model (LVM) whose transformation

function is parameterized by an encoder-decoder framework, where the prior high-performance prediction model comes in. By bringing in a latent variable model as an ancestral sampler to approximate or initialize the MCMC computational process for efficient sampling, the EBM can be learned efficiently. The energy function in the EBM, in turn, can be used to refine the LVM’s samples, achieving a coarse-to-fine generative saliency detection.

Moreover, based on the conditional cooperative network, we propose a novel *cooperative learning while cooperative recovering* strategy for weakly supervised saliency learning, in which we learn our model from incomplete data, where each training image is associated with a partially observed annotation (*e.g.*, scribble [62]). At each learning iteration, the incomplete saliency ground truth is firstly recovered in the low-dimensional latent space of the latent variable model via inference, and then refined by pushing it to the local mode in the energy landscape of the energy-based model. The recovered saliency maps are treated as pseudo labels to train the proposed framework.

In experiments, we demonstrate that our model not only can achieve state-of-the-art performance in both fully supervised and weakly supervised saliency prediction, but also can produce stochastic predictions representing the sampling process of visual saliency. Furthermore, we show that the learned energy function of the EBM can serve as a pre-trained “cost function” to refine the results from any saliency prediction models. It is worth noting that, although [60] used an LVM to model labeling variants, they directly find a local minima with the LVM. Going beyond, this work further searches in the neighbourhood of the local minima with an EBM to obtain a better prediction. Another work that is close to us is [61], which adopted an LVM for noise estimation. However, it cannot directly recover the missing labels with partial supervision, *e.g.* scribble annotation.

Our main contributions can be summarized as:

1. We study the generative modeling of saliency prediction, and formulate this problem in the frameworks of EBM and LVM (See Sections 3.1 and 3.2), which is a new angle to model and solve the saliency prediction problem.
2. We propose a generative cooperative saliency prediction framework, *SalCoopNets*, which jointly trains the LVM predictor and the EBM predictor in a cooperative learning scheme to offer reliable and efficient saliency prediction. (See Algorithm 1).
3. We generalize our method to weakly supervised saliency prediction scenarios with incomplete annotations by proposing the *cooperative learning while recovering* algorithm (Algorithm 2), in which we train the model and simultaneously recover the unlabeled area.
4. We show that, the learned energy function in our model can serve as a refinement module to refine the predictions from other saliency predictors. (See Section 6.3).

5. We provide empirical results in both fully and weakly supervised settings to corroborate our framework.

2. Related Work

Fully/Weakly Supervised Saliency Models. Existing fully supervised saliency prediction models [38, 25, 27, 42, 24, 33, 46, 45, 40, 39, 43] mainly focus on exploring image context information and generating structure-preserving predictions. [46, 39, 40, 38, 25, 24, 45] introduced saliency prediction models by effectively integrating higher- and lower-level features. [42, 27, 43] proposed edge-aware loss term to penalize errors along object boundaries. Note that all the above models are deterministic models. Recently, [60] introduced a conditional variational auto-encoder [17, 15] for stochastic RGB-D saliency detection. Similarly, we introduce a cooperative learning pipeline to achieve probabilistic coarse-to-fine RGB saliency detection via a latent variable model. However, [60] does not have a “fine” model, and this is the first time an energy-based model has been used for probabilistic saliency detection.

The weakly supervised saliency models [37, 21, 30, 62] learn saliency from easy-to-obtain weak labels, including image-level labels [37, 22], noisy labels [30, 63, 59] or partial scribble labels [62]. Although a probabilistic model was explored in [61], they used a generative model for noise modeling. In this paper, for the weakly supervised task, we use a latent variable to model the distribution of the hidden clean saliency map.

Generative Cooperative Networks. Deep energy-based generative models [48], with energy functions parameterized by modern convolutional neural networks, have gained significant attention in modeling probability density of high-dimensional data. Successful applications in computer vision include image generation [48, 7, 31], video generation [53, 54], 3D volumetric shape generation [51, 50], and unordered point cloud generation [49]. The maximum likelihood learning of the energy-based model typically requires iterative MCMC sampling, which is computationally challenging. To relieve the computational burden of MCMC, the Generative Cooperative Networks (CoopNets) in [47] propose to learn a separate latent variable model (*i.e.* a generator) to serve as an efficient approximate sampler for training the energy-based model. [52] proposes a variant of CoopNets by replacing the generator with a variational auto-encoder (VAE) [16]. Our paper proposes a conditional model under the cooperative learning framework for visual saliency prediction. Our solution can be treated as a conditional version of [47]. While differently, we also generalize our model to weakly supervised learning by proposing a *cooperative learning while recovering* algorithm. In this way, we can learn the model from incomplete data for weakly supervised saliency prediction.

Conditional Deep Generative Models. Our framework be-

longs to the family of conditional generative models, which also include conditional generative adversarial networks (CGANs) [28] and conditional variational auto-encoders (CVAEs) [34]. Different from existing CGAN-based conditional generative models [26, 64, 55, 32, 58, 12, 36], which use GANs to detect higher-order inconsistency between ground truth and the prediction, or CVAEs based models [19, 60] in which a latent variable model representing an implicit density is learned, our model learns an explicit density via energy-based modeling. More importantly, our model allows an additional refinement for the latent variable model during prediction, which is sorely lacking in both CGANs and CVAEs frameworks.

3. Generative Cooperative Saliency Prediction

In this section, we propose a novel saliency prediction approach based on training an energy-based model (EBM) and a latent variable model (LVM) in a generative cooperative manner. The resulting prediction process is accomplished by cooperative sampling from both learned models. We will first introduce how to model the saliency prediction problem by using the frameworks of energy-based model and latent variable model in sections 3.1 and 3.2, respectively. Then we will discuss how to combine these two models to offer the best of both worlds for saliency prediction in section 3.3. The training strategy and the details of network design will be presented in sections 3.4 and 5.1.

3.1. EBM as a Fine but Slow Predictor

Let X be an image, and Y be its saliency map. The energy-based model $p_\theta(Y|X)$ defines a distribution of saliency Y given an image X by

$$p_\theta(Y|X) = \frac{p_\theta(Y, X)}{\int p_\theta(Y, X) dY} = \frac{1}{Z(X; \theta)} \exp[-U_\theta(Y, X)], \quad (1)$$

where the energy function $U_\theta(Y, X)$, parameterized by a bottom-up neural network, maps the input image-saliency pair to a scalar, and θ represents the network parameters. $Z(X; \theta) = \int \exp[-U_\theta(Y, X)] dY$ is the normalizing constant. When U_θ is learned and an image X is given, the prediction of saliency Y can be achieved by Langevin sampling [29] $Y \sim p_\theta(Y|X)$, which makes use of the gradient of the energy function and iterates the following step:

$$Y_{\tau+1} = Y_\tau - \frac{\delta^2}{2} \frac{\partial U_\theta(Y_\tau, X)}{\partial Y} + \delta \Delta_\tau, \Delta_\tau \sim N(0, I_D), \quad (2)$$

where τ indexes the Langevin time steps, and δ is the step size. The Langevin dynamics [29] is equivalent to a stochastic gradient descent algorithm that seeks to find the minimum of the objective function defined by $U_\theta(Y, X)$. The Gaussian noise term Δ_τ is a Brownian motion that prevents the gradient descent from being trapped by local minima of

$U_\theta(Y, X)$. The energy function $U_\theta(Y, X)$ in Eq.(1) can be regarded as a trainable cost function of the task of saliency prediction, while the prediction process via Langevin dynamics in Eq.(2) can be considered as finding Y to minimize the cost $U_\theta(Y, X)$ given input X . Such a framework can learn reliable and generalizable cost function for saliency prediction. However, due to the iterative sampling process, EBM is a slow but fine saliency predictor.

3.2. LVM as a Coarse but Fast Predictor

Let h be a latent Gaussian noise vector, $G_\alpha(X, h)$ be a mapping function parameterized by a noise-injected encoder-decoder network with skip connections. α contains all the learning parameters in the network. The latent variable model is given by:

$$h \sim N(0, I_d), Y = G_\alpha(X, h) + \epsilon, \epsilon \sim N(0, \sigma^2 I_D), \quad (3)$$

which defines an implicit conditional distribution of saliency Y given an image X , *i.e.*, $p_\alpha(Y|X) = \int p(h) p_\alpha(Y|X, h) dh$, where $p_\alpha(Y|X, h) = N(G_\alpha(X, h), \sigma^2 I_D)$. The saliency prediction can be achieved by an ancestral sampling by first sampling an injected Gaussian white noise h and then transforming the noise and the image X to a saliency map Y . Since the ancestral sampling is a direct mapping, which is faster than the iterative Langevin dynamics. However, without a cost function as in EBM, the learned mapping in this model is hard to be generalized to a new domain.

3.3. Cooperative Prediction with Two Predictors

We propose to predict the saliency of an image by a cooperative sampling strategy, where we first use the coarse saliency predictor to generate an initial prediction \hat{Y} via a non-iterative ancestral sampling, and then we use the fine saliency predictor to refine the initial prediction via iterative Langevin revision to obtain the revised saliency \tilde{Y} , *i.e.*,

$$\begin{aligned} \hat{Y} &= G_\alpha(X, \hat{h}), \hat{h} \sim N(0, I_d), \\ \tilde{Y}_{\tau+1} &= \tilde{Y}_\tau - \frac{\delta^2}{2} \frac{\partial U_\theta(\tilde{Y}_\tau, X)}{\partial \tilde{Y}} + \delta N(0, I_D), \tilde{Y}_0 = \hat{Y}. \end{aligned} \quad (4)$$

We call this cooperative sampling based coarse-to-fine prediction. In this way, we take both advantages of these two saliency predictors in the sense that the fine saliency predictor (*i.e.*, Langevin sampler) is initialized by the efficient coarse saliency predictor (*i.e.*, ancestral sampler), while the coarse saliency predictor is refined by the accurate fine saliency predictor that aims to minimize a cost function U_θ .

Since our conditional model represents a stochastic mapping, the prediction is stochastic as well. To evaluate the learned model on saliency prediction tasks, we can draw multiple h 's from the prior $N(0, I_d)$ and use their average

to generate \hat{Y} , then a Langevin dynamics with noise disabled (*i.e.*, gradient descent) is performed to push \hat{Y} to its nearest local minimum \tilde{Y} based on the learned energy function. The resulting \tilde{Y} is treated as a prediction of our model.

3.4. Cooperative Training of Two Predictors

We use the cooperative training method to learn the parameters (θ, α) of the two predictors. At each iteration, the algorithm first generates the synthetic examples via the cooperative sampling strategy shown in Eq.(4), and then use the synthetic examples to compute the gradients to update both predictors. We present the update formula of each predictor below.

MCMC-based Maximum Likelihood Estimation of Fine Saliency Predictor. Given a training dataset $\{(X_i, Y_i)\}_{i=1}^n$, we train the fine saliency predictor via maximum likelihood estimation, which maximizes the log-likelihood of the data $L(\theta) = \frac{1}{n} \sum_{i=1}^n \log p_\theta(Y_i|X_i)$, whose gradient $\Delta\theta = \frac{1}{n} \sum_{i=1}^n \{E_{p_\theta(Y|X_i)}[\frac{\partial}{\partial\theta} U_\theta(Y, X_i)] - \frac{\partial}{\partial\theta} U_\theta(Y_i, X_i)\}$. We rely on the cooperative sampling in Eq.(4) to sample $\tilde{Y}_i \sim p_\theta(Y|X_i)$ to approximate the gradient:

$$\Delta\theta \approx \frac{1}{n} \sum_{i=1}^n \frac{\partial}{\partial\theta} U_\theta(\tilde{Y}_i, X_i) - \frac{1}{n} \sum_{i=1}^n \frac{\partial}{\partial\theta} U_\theta(Y_i, X_i). \quad (5)$$

We can use Adam with $\Delta\theta$ to update θ . We denote $\Delta\theta(\{Y_i\}, \{\tilde{Y}_i\})$ as a function of $\{Y_i\}$ and $\{\tilde{Y}_i\}$.

Maximum Likelihood Training of Coarse Saliency Predictor by MCMC Teaching. Even though the fine saliency predictor learns from the training data, the coarse saliency predictor learns to catch up with the fine saliency predictor by treating $\{(X, \tilde{Y})\}_{i=1}^n$ as training examples. The learning objective is to maximize the log-likelihood of the samples drawn from $p_\theta(Y|X)$, *i.e.*, $L(\alpha) = \frac{1}{n} \sum_{i=1}^n \log p_\alpha(\tilde{Y}_i|X_i)$, whose gradient can be computed by

$$\Delta\alpha = \sum_{i=1}^n E_{h \sim p_\alpha(h|Y_i, X_i)} \left[\frac{\partial}{\partial\alpha} \log p_\alpha(Y_i, h|X_i) \right]. \quad (6)$$

This leads to an MCMC-based solution that iterates (i) an inference step: inferring latent \tilde{h} by sampling from posterior distribution $h \sim p_\alpha(h|Y, X)$ via Langevin dynamics, which iterates the following:

$$h_{\tau+1} = h_\tau + \frac{\delta^2}{2} \frac{\partial}{\partial h} \log p_\alpha(Y, h_\tau|X) + \delta \Delta_\tau, \quad (7)$$

where $\Delta_\tau \sim N(0, I_d)$, $\frac{\partial}{\partial h} \log p_\alpha(Y, h_\tau|X) = \frac{1}{\sigma^2} (Y - G_\alpha(X, h_\tau)) \frac{\partial}{\partial h} G_\alpha(X, h_\tau) - h_\tau$, and (ii) a learning step: with $\{\tilde{h}_i, \tilde{Y}_i, X_i\}$, we update α via Adam optimizer with

$$\Delta\alpha \approx \frac{1}{n} \sum_{i=1}^n \frac{1}{\sigma^2} (\tilde{Y}_i - G_\alpha(X_i, \tilde{h}_i)) \frac{\partial}{\partial\alpha} G_\alpha(X_i, \tilde{h}_i). \quad (8)$$

Algorithm 1 Training algorithm for Cooperative Saliency Predictor

Input:

- (1) Training images $\{X_i\}_i^n$ with associated saliency maps $\{Y_i\}_i^n$;
- (2) maximal number of learning iterations T .

Output: Parameters θ and α

- 1: Initialize θ and α
 - 2: **for** $t \leftarrow 1$ to T **do**
 - 3: Draw $\hat{h}_i \sim N(0, I_d)$
 - 4: Sample initial prediction $\hat{Y}_i = G_\alpha(X_i, \hat{h}_i)$.
 - 5: Revise \hat{Y}_i to obtain \tilde{Y}_i by Langevin in Eq. (2)
 - 6: Revise \hat{h}_i to obtain \tilde{h}_i by Langevin in Eq. (7)
 - 7: Update θ with $\Delta\theta(\{Y_i\}, \{\tilde{Y}_i\})$ in Eq.(5) using Adam
 - 8: Update α with $\Delta\alpha(\{\tilde{h}_i\}, \{\tilde{Y}_i\})$ in Eq.(8) using Adam
 - 9: **end for**
-

Algorithm 2 Learning while recovering

Input:

- (1) Images $\{X_i\}_i^n$ with incomplete annotations $\{Y'_i\}_i^n$;
- (2) Number of learning iterations T

Output: Parameters θ and α

- 1: Initialize θ and α
 - 2: **for** $t \leftarrow 1$ to T **do**
 - 3: Infer \hat{h}'_i from the visible part of Y'_i by Langevin dynamics in Eq. (7)
 - 4: Obtain initial recovery $\hat{Y}_i = G_\alpha(X_i, \hat{h}'_i)$.
 - 5: Revise \hat{Y}'_i to obtain \tilde{Y}'_i by Langevin in Eq. (2)
 - 6: Draw $\hat{h}_i \sim N(0, I_d)$
 - 7: Sample initial prediction $\hat{Y}_i = G_\alpha(X_i, \hat{h}_i)$.
 - 8: Revise \hat{Y}_i to obtain \tilde{Y}_i by Langevin in Eq. (2)
 - 9: Revise \hat{h}_i to obtain \tilde{h}_i by Langevin in Eq. (7)
 - 10: Update θ with $\Delta\theta(\{\tilde{Y}'_i\}, \{\tilde{Y}_i\})$ using Adam
 - 11: Update α with $\Delta\alpha(\{\tilde{h}_i\}, \{\tilde{Y}_i\})$ using Adam
 - 12: **end for**
-

Since G_α is parameterized by a differentiable neural network, both $\frac{\partial}{\partial h} G_\alpha(X, h_\tau)$ in Eq.(7) and $\frac{\partial}{\partial \alpha} G_\alpha(X_i, \tilde{h}_i)$ in Eq.(8) can be efficiently computed by back-propagation. We denote $\Delta\alpha(\{\tilde{h}_i\}, \{\tilde{Y}_i\})$ as a function of $\{\tilde{h}_i\}$ and $\{\tilde{Y}_i\}$. Algorithm 1 presents a description of the cooperative learning algorithm of the fine and coarse saliency predictors.

4. Weakly Supervised Saliency Prediction

Our model can be learned from a partially-observed training dataset $D' = \{(X_i, Y'_i)\}_{i=1}^n$, where only partial pixel-wise annotation is available, *e.g.*, scribble [62]. Algorithm 2 describes the basic pipeline.

Recovery by Coarse Saliency Predictor in Latent Space. Given an image X_i and its incomplete saliency map Y'_i , the recovery of the missing part of Y'_i can be achieved by first inferring the latent variable h'_i based on partially observed saliency information via $h'_i \sim p_\alpha(h|Y'_i, X_i)$, and then generating $\hat{Y}'_i = G_\alpha(X_i, h'_i)$ with the inferred h'_i .

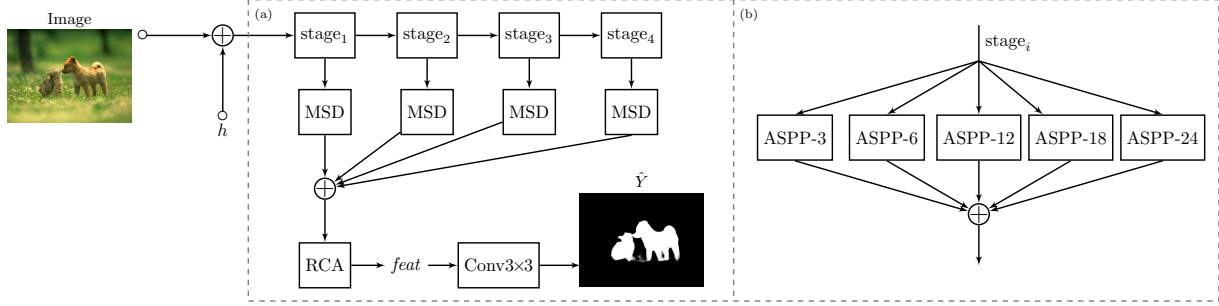


Figure 1: Network structure of the latent variable network. \oplus denotes the vector concatenation operation. (a) Overall structure. $\text{stage}_1, \dots, \text{stage}_4$ are four convolutional blocks of the backbone network ResNet50 [11]. “RCA” is the residual channel attention module in [65]. (b) Basic structure of Multi-scale Dilation Network (MSD). Each $\text{ASPP-}r$ ($r = \{3, 6, 12, 18, 24\}$) is an Atrous Spatial Pyramid Pooling [1] module.

Let O_i be a binary mask, with the same size as Y'_i , indicating the locations of visible annotations in Y'_i . O_i varies for different Y'_i and can be extracted from Y'_i . The Langevin dynamics for recovery iterates the same step in Eq.(7) except that $\frac{\partial}{\partial h} \log p_\alpha(Y', h_\tau | X) = \frac{1}{\sigma^2} (O \circ (Y - G_\alpha(X, h_\tau))) \frac{\partial}{\partial h} G_\alpha(X, h_\tau) - h_\tau$, where $\text{sign} \circ$ denotes element-wise matrix multiplication operation.

Recovery by Fine Saliency Predictor in Energy Landscape. With the initial recovered result \hat{Y}' by the coarse saliency predictor p_α , the fine saliency predictor p_θ can further recover the result by running finite steps of Langevin dynamics in Eq.(2) initialized from \hat{Y}' and obtain \tilde{Y}' . The underlying principle is that the initial recovery \hat{Y}' might be just around the local modes of the energy function. A few steps of Langevin dynamics (*i.e.*, stochastic gradient descent) of p_θ , starting from \hat{Y}' , will push \hat{Y}' to its nearby low energy mode, in which its potential fully observed version Y_i could be.

Cooperative Learning while Cooperative Recovering. At each iteration t , we perform the above cooperative recovery of the training saliency map $\{Y'\}_{i=1}^n$ via $p_{\theta(t)}$ and $p_{\alpha(t)}$, while learning $p_{\theta(t+1)}$ and $p_{\alpha(t+1)}$ from $\{X_i, \tilde{Y}'^{(t)}_i\}_{i=1}^n$, where $\tilde{Y}'^{(t)}_i$ is the recovered saliency map at t -th iteration. The parameter θ is still updated via Eq.(5) except that we replace Y_i by \tilde{Y}'_i . That is, at each iteration, we use the recovered \tilde{Y}'_i , instead of the original Y_i , along with \tilde{Y}_i to compute the gradient of log-likelihood, which is denoted by $\Delta\theta(\{\tilde{Y}'_i\}, \{\tilde{Y}_i\})$. The algorithm simultaneously performs (i) cooperative recovering of missing annotations; (ii) cooperative sampling to generate annotations; (iii) cooperative learning of the two models by updating parameters with both recovered annotations and generated annotations.

5. Technical Details

5.1. Network Architecture

Latent Variable Model: The latent variable model $G_\alpha(X, h)$ maps the concatenation of image X and latent variable h (we expand h to same spatial size of X) to a coarse saliency map \hat{Y} as shown in Fig. 1. We follow pioneer saliency detection works [45, 33, 42, 46] to address two major issues of saliency models: structure recovery solution and multi-scale strategy. To solve the first problem, we adopt structure aware similarity as in [42] to further penalize errors near edges of the prediction in training the latent variable model. To achieve multi-scale saliency detection, we design an encoder-decoder based network with ResNet50 [11] as backbone. We first design a Multi-scale Dilation Network (MSD), shown in Fig. 1 (b), with gradually enlarged dilation rates to capture different scales of context information. Then the output features are concatenated and fed to the “Residual Channel Attention” (RCA) module [65] to obtain a discriminative feature representation. Finally, one 3×3 convolutional layer is adopted to map the feature to a one-channel saliency map \hat{Y} .

Energy Function: The energy function $U_\theta(Y, X)$ represents the energy of input pair. Let $\text{c}\underline{k}\text{s}\underline{l}-\underline{n}$ denote a $k \times k$ Convolution-BatchNorm-RELU layer with n filters and stride l , $\text{fc}-\underline{n}$ a fully connected layer with n filters. The energy network is composed of: $\text{c}3\text{s}1-32$, $\text{c}4\text{s}2-64$, $\text{c}4\text{s}2-128$, $\text{c}4\text{s}2-256$, $\text{c}4\text{s}1-1$, $\text{fc}-100$.

5.2. Implementation Details

We trained our model using PyTorch with a maximum of 30 epochs. Each image is rescaled to 352×352 . ResNet50 [11] is chosen as backbone of the latent variable model. Empirically, we set the dimension of the latent space as $h = 8$. The learning rates of the latent variable model and EBM function are initialized to $1e-4$ and $1e-3$ respectively.

We used Adam optimizer with momentum 0.9 and decrease the learning rate 10% after 20 epochs. It took 20 hours of training with batch size 7 using a single NVIDIA GeForce RTX 2080Ti GPU.

6. Experiments

Datasets: We used the DUTS dataset [37] for training the fully supervised model, and scribble annotation S-DUTS [62] for training the weakly supervised model. Testing images include 1) DUTS testing dataset, 2) ECSSD [56], 3) DUT [57], 4) HKU-IS [23], 5) THUR [2] and SOC [3].

Compared methods: We compared our method against eleven state-of-the-art fully supervised deep saliency detection methods: DGRL [38], PiCANet [25], F3Net [42], NLDF [27], PoolNet [24], BASNet [33], AFNet [6], MSNet [44], SCRNet [46], ITSD [66] and LDF [43]. We also compare our weakly supervised solution in Section 4 with the scribble saliency detection model SSAL [62].

Evaluation Metrics: We evaluate performance of ours and compared methods with four saliency evaluation metrics, including: Mean Absolute Error (\mathcal{M}), mean F-measure (F_β), mean E-measure (E_ξ) [5] and S-measure (S_α) [4]. We introduce these evaluation metrics in detail in the supplementary materials.

6.1. Comparison with Fully-supervised Models

Quantitative comparison: We evaluate performance of compared methods and ours and show results in Table 1, where “Ours” in the “Deep Fully Supervised Models” is the proposed fully supervised solution in Algorithm 1. We observe consistent performance improvement of “Ours” over four testing datasets compared with benchmark models. LDF [43] achieves comparable performance as ours in the DUTS testing dataset [37]. The main reason is that there exists an extra edge detection branch in [37] to constrain the accuracy of prediction along object edges. This inspires us to further explore edge related constraint in the future. For the SOC dataset, 33% of the images are pure texture images without obvious salient region. The ground truth is then defined as an all-zeros matrix, indicating all background areas. However, we can still observe some salient patterns in these images. We will investigate this dataset in the future.

We also designed two alternative generator network based saliency detection pipelines with CVAEs [35] and CGANs [28] respectively (details about these two alternative network are introduced in Section 6.5, and performance is shown as “CVAE” and “CGAN”. As indicated in both Table 1 and our experience of training, we found that the CGANs-based model is very sensitive to the weights of the discriminator loss, and the whole training is not very stable. The CVAEs-based model can achieve stable training, while imbalanced training (generator model and inference

model) may lead to posterior collapse [10], where the network fails to model the sampling process of visual saliency. The performance gap between ours and alternative generator networks validates our superior performance.

Qualitative comparison: As a generative model, we intend to model sampling process of visual saliency, thus, diversity of prediction is a main standard to evaluate performance of our model. We visualize predictions of ours and two competing methods (F3Net and SCRNet) as shown in Fig. 2, where “Our Samples” represent our predictions with four iterations of sampling, and “Ours” is computed with an average of multiple latent variable h as input (introduced in Section 3). Fig. 2 shows that the deterministic one-to-one mapping may over-confidently segment too many or too few regions as salient. The proposed solution can produce multiple predictions with each iteration of sampling, which is more consistent with the “subjective” nature of saliency. Furthermore, as shown in the “Ours” column, when taking the average of latent variable h as input, we can produce predictions that are most similar to the provided ground truth compared with the competing methods.

6.2. Weakly Supervised Saliency Detection

We extend our solution to weakly supervised saliency detection with scribble annotation [62]. As shown in Fig. 3 (a), compared with the fully annotated ground truth (“GT”), scribble annotation (“Scribble”) is sparse (orange scribble is salient region, and blue scribble represents background). With the proposed “cooperative learning while recovering” strategy, we can recover the missing annotation regions as shown in “Rec-ed”. Different from [62], which incorporates an extra edge detection module and smoothness loss [41] to push the prediction to share similar shape to the input image, we instead put the smoothness constraint into the energy-based model while updating the parameter set θ in Eq. 5. “Ours” in Tab. 1 in the “Weakly Supervised Models” section is our weakly supervised learning model. Note that, the scribble annotation is only used during training as partial supervision. During testing, given an input image, we can produce stochastic predictions as shown in Fig. 3 (b).

We note that [61] used a latent variable model to learn from the noisy label. Given the scribble annotation, we refine the noisy label using a DenseCRF [1] to obtain a noisy saliency map. Then, we follow [61] and train a weakly supervised model with [61]. The performance is shown as “NED” in Table 1. We observe inferior performance of “NED” compared with both “SSAL” and our results. The main reason is that the implementation of “NED” is designed for noisy labels rather than weak supervision, and as expected it does not perform well in our weak setting.

Table 1: Performance comparison with benchmark saliency prediction models.

Method	DUTS [37]				ECSSD [56]				DUT [57]				HKU-IS [23]				THUR [2]				SOC [3]			
	$S_\alpha \uparrow$	$F_\beta \uparrow$	$E_\xi \uparrow$	$\mathcal{M} \downarrow$	$S_\alpha \uparrow$	$F_\beta \uparrow$	$E_\xi \uparrow$	$\mathcal{M} \downarrow$	$S_\alpha \uparrow$	$F_\beta \uparrow$	$E_\xi \uparrow$	$\mathcal{M} \downarrow$	$S_\alpha \uparrow$	$F_\beta \uparrow$	$E_\xi \uparrow$	$\mathcal{M} \downarrow$	$S_\alpha \uparrow$	$F_\beta \uparrow$	$E_\xi \uparrow$	$\mathcal{M} \downarrow$	$S_\alpha \uparrow$	$F_\beta \uparrow$	$E_\xi \uparrow$	$\mathcal{M} \downarrow$
Deep Fully Supervised Models																								
DGRL [38]	.846	.790	.887	.051	.902	.898	.934	.045	.809	.726	.845	.063	.897	.884	.939	.037	.816	.727	.838	.077	.791	.348	.820	.137
PiCAN [25]	.842	.757	.853	.062	.898	.872	.909	.054	.817	.711	.823	.072	.895	.854	.910	.046	.818	.710	.821	.084	.801	.332	.810	.133
F3Net [42]	.888	.852	.920	.035	.919	.921	.943	.036	.839	.766	.864	.053	.917	.910	.952	.028	.838	.761	.858	.066	.828	.340	.846	.098
NLDF [27]	.816	.757	.851	.065	.870	.871	.896	.066	.770	.683	.798	.080	.879	.871	.914	.048	.801	.711	.827	.081	.816	.319	.837	.106
PoolN [24]	.887	.840	.910	.037	.919	.913	.938	.038	.831	.748	.848	.054	.919	.903	.945	.030	.834	.745	.850	.070	.829	.355	.846	.098
BASN [33]	.876	.823	.896	.048	.910	.913	.938	.040	.836	.767	.865	.057	.909	.903	.943	.032	.823	.737	.841	.073	.841	.359	.864	.092
AFNet [6]	.867	.812	.893	.046	.907	.901	.929	.045	.826	.743	.846	.057	.905	.888	.934	.036	.825	.733	.840	.072	.700	.312	.684	.115
MSNet [44]	.862	.792	.883	.049	.905	.886	.922	.048	.809	.710	.831	.064	.907	.878	.930	.039	.819	.718	.829	.079	-	-	-	-
SCRN [46]	.885	.833	.900	.040	.920	.910	.933	.041	.837	.749	.847	.056	.916	.894	.935	.034	.845	.758	.858	.066	.838	.363	.859	.099
ITSD [66]	.885	.840	.913	.041	.919	.917	.941	.037	.840	.768	.865	.061	.917	.904	.947	.031	.836	.753	.852	.070	.773	.361	.792	.166
LDF [43]	.892	.861	.925	.034	.919	.923	.943	.036	.839	.770	.865	.052	.920	.913	.953	.028	.842	.768	.863	.064	.835	.369	.856	.103
SalCoopNets	.890	.856	.924	.034	.926	.930	.954	.031	.852	.788	.879	.046	.923	.917	.957	.026	.847	.771	.867	.061	.839	.368	.860	.092
Weakly Supervised Models																								
SSAL [62]	.803	.747	.865	.062	.863	.865	.908	.061	.785	.702	.835	.068	.865	.858	.923	.047	.800	.718	.837	.077	.804	.309	.793	.143
NED [61]	.796	.732	.829	.067	.852	.849	.871	.071	.782	.694	.810	.074	.861	.852	.904	.048	.800	.713	.830	.079	.783	.300	.791	.153
SalCoopNets	.813	.755	.863	.059	.872	.874	.910	.060	.791	.707	.840	.061	.871	.859	.929	.042	.804	.717	.839	.074	.812	.314	.806	.137
Alternative Generator Models																								
CVAE	.866	.824	.900	.041	.906	.910	.932	.043	.816	.737	.844	.055	.910	.903	.943	.032	.835	.755	.859	.065	.843	.361	.866	.098
CGAN	.846	.785	.883	.049	.900	.895	.928	.047	.799	.705	.828	.063	.894	.875	.930	.039	.823	.732	.850	.071	.841	.362	.859	.103

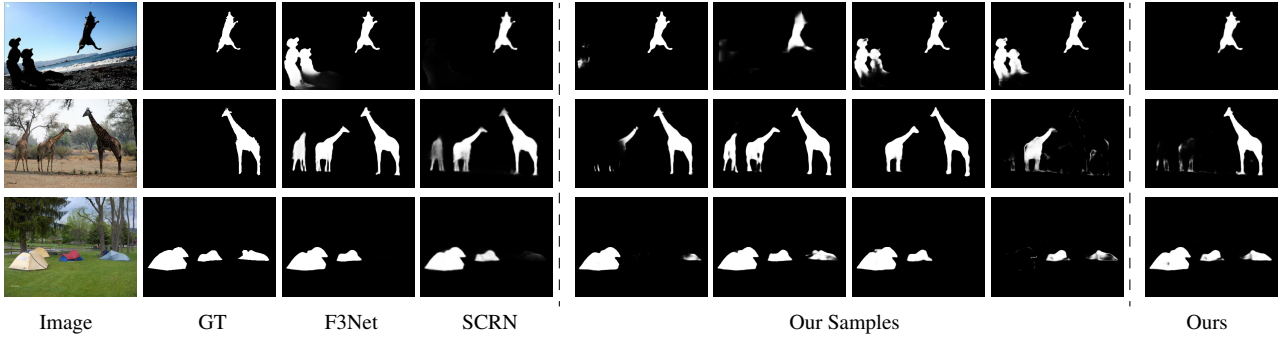


Figure 2: Visual comparison of predictions of the SalCoopNets and competing saliency models.

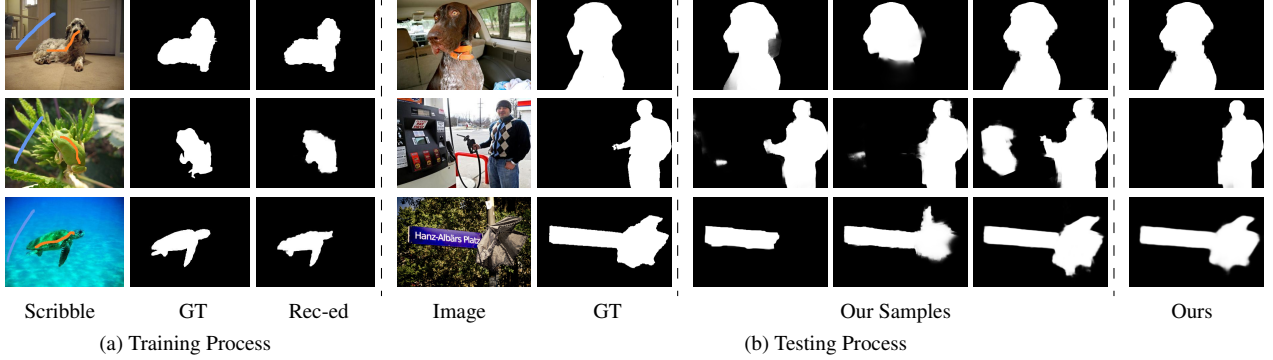


Figure 3: Examples showing the training and testing related data of our “cooperative learning while recovering” weakly supervised learning solution. Note that, scribble is only used during training stage.

6.3. Energy Function as a Refinement Module

As shown in Eq. 2, the energy-based model can iteratively refine the prediction with Langevin sampling. With the trained EBM, we use it to refine predictions from ex-

isting deep saliency detection models. Performance is shown in Table 2. “NLDF_R”, “SCRN_R” “BASN_R” and “PoolN_R”, representing using EBM to refine NLDF

Table 2: Performance comparison of ablation study related models.

	DUTS [37]				ECSSD [56]				DUT [57]				HKU-IS [23]				THUR [2]				SOC [3]			
	$S_\alpha \uparrow$	$F_\beta \uparrow$	$E_\xi \uparrow$	$\mathcal{M} \downarrow$	$S_\alpha \uparrow$	$F_\beta \uparrow$	$E_\xi \uparrow$	$\mathcal{M} \downarrow$	$S_\alpha \uparrow$	$F_\beta \uparrow$	$E_\xi \uparrow$	$\mathcal{M} \downarrow$	$S_\alpha \uparrow$	$F_\beta \uparrow$	$E_\xi \uparrow$	$\mathcal{M} \downarrow$	$S_\alpha \uparrow$	$F_\beta \uparrow$	$E_\xi \uparrow$	$\mathcal{M} \downarrow$	$S_\alpha \uparrow$	$F_\beta \uparrow$	$E_\xi \uparrow$	$\mathcal{M} \downarrow$
Original Performance of Compared Methods																								
NLDF [27]	.816	.757	.851	.065	.870	.871	.896	.066	.770	.683	.798	.080	.879	.871	.914	.048	.801	.711	.827	.081	.816	.319	.837	.106
PoolN [24]	.887	.840	.910	.037	.919	.913	.938	.038	.831	.748	.848	.054	.919	.903	.945	.030	.834	.745	.850	.070	.829	.355	.846	.098
BASN [33]	.876	.823	.896	.048	.910	.913	.938	.040	.836	.767	.865	.057	.909	.903	.943	.032	.823	.737	.841	.073	.841	.359	.864	.092
SCRN [46]	.885	.833	.900	.040	.920	.910	.933	.041	.837	.749	.847	.056	.916	.894	.935	.034	.845	.758	.858	.066	.838	.363	.859	.099
EBM as Refinement Module																								
NLDF_R	.867	.827	.911	.040	.906	.911	.939	.041	.814	.738	.850	.058	.909	.903	.951	.030	.827	.747	.854	.068	.812	.327	.825	.132
PoolN_R	.890	.852	.921	.035	.923	.920	.945	.036	.840	.766	.867	.050	.925	.914	.952	.027	.834	.745	.850	.070	.829	.355	.846	.106
BASN_R	.882	.836	.893	.042	.923	.919	.944	.035	.843	.788	.875	.050	.913	.914	.950	.030	.834	.745	.850	.071	.841	.359	.864	.092
SCRN_R	.887	.854	.922	.035	.923	.923	.944	.036	.839	.759	.861	.052	.919	.913	.953	.028	.849	.763	.863	.064	.846	.369	.868	.091
Ablation Study																								
DGen	.872	.832	.917	.038	.909	.911	.940	.040	.820	.745	.857	.055	.911	.903	.952	.030	.828	.748	.855	.068	.832	.359	.852	.101
SGen	.881	.849	.920	.036	.918	.923	.946	.036	.834	.766	.865	.052	.918	.914	.954	.027	.833	.756	.856	.068	.835	.362	.864	.095
DEBM	.883	.851	.921	.035	.916	.920	.944	.036	.835	.769	.866	.050	.919	.915	.955	.026	.833	.757	.858	.064	.841	.367	.870	.096
CRFs	.880	.842	.925	.036	.905	.909	.931	.042	.826	.739	.853	.056	.910	.914	.957	.031	.837	.769	.862	.066	.842	.363	.865	.094
SalCoopNets	.890	.856	.924	.034	.926	.930	.954	.031	.852	.788	.879	.046	.923	.917	.957	.026	.847	.771	.867	.061	.839	.368	.860	.092

[27], SCR N [46], BASN [33] and PoolN [24] respectively¹. Compared with the original performance of these models, we observe consistent performance improvement with EBM as a refinement module, especially for NLDF, we achieve around 5% performance improvement for S-measure, F-measure and E-measure, and 2% performance improvement for MAE. We further show three examples of those models with and without EBM as refinement in Fig. 6. Both performance improvement and visual comparison illustrates the effectiveness of EBM as a refinement module.

6.4. Ablation Study

We carried out the following experiments as shown in Table 2 to further analyse our solution.

Training the deterministic latent variable model: G_α can be trained directly without the latent variable h , i.e. $G_\alpha(X)$, and the result is shown as “DGen”. We observe competing performance of “DGen” compared with existing benchmark fully supervised saliency detection models. While, the gap between “DGen” and “Ours” illustrates superior performance of the proposed solution.

Training directly the latent variable model: We treat the stochastic saliency encoder-decoder $G_\alpha(X, h)$ as our final model, where the latent variable h is updated through Langevin dynamics as shown in Eq. 7. In this way, our method performs alternating back-propagation [9]. The result is shown in “SGen”. Compared with “DGen”, “SGen” achieves better performance, which illustrates effectiveness of the latent variable model.

Training the deterministic latent variable model with EBM as refinement: We add EBM to “DGen” as a refinement module during both training and testing. The result is shown in “DEBM”. The gap between “DEBM”

¹We choose these four models due to their accessible codes and saliency maps

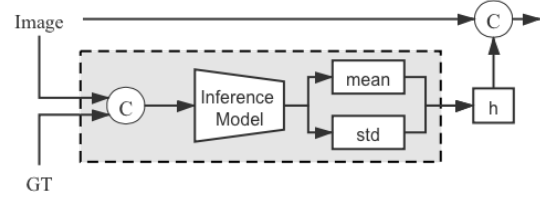


Figure 4: Network structure for training a CVAE based saliency prediction network.

and “DGen” is consistent with EBM as refinement of pre-trained saliency models in Section 6.3, which further proves feasibility of EBM as saliency refinement module.

Refine the latent variable model with CRFs[1]: As a popular post-processing technique, dense CRFs [1] can be adopted to refine predictions of our latent variable model. We refine “DGen” with the dense CRFs, and show its performance as “CRFs” in Table 2. We observe unstable performance of “CRFs”, and the main reason for this is the difficulty in finding the effective hyper parameters. In order to find the right hyper parameter set, [18] introduced the trainable CRFs, which is just similar to our trainable EBM.

6.5. Alternative Generative Models

We further investigate alternative generative models for saliency detection, and design two extra stochastic RGB saliency detection framework by using CVAEs [34] and CGANs [28].

Learning RGB Saliency via CVAEs:

A CVAE [35] is a conditional directed graph model, which includes three variables, the input X or conditional variable that modulates the prior on Gaussian latent variable

Table 3: Network structure of the inference model in CVAEs based saliency prediction framework.

Input Channel	Output Channel	kernel size	Stride	Padding
4	32	4	2	1
32	64	4	2	1
64	128	4	2	1
128	256	4	2	1
256	256	4	2	1
32*8*11*11	8	-	-	-
32*8*11*11	8	-	-	-

h and generates the output prediction Y . Two main modules are included in a conventional CVAE based framework: a generator model $p_\theta(Y|X, h)$, which generates prediction Y with input X and h as input, and an inference model $p_\theta(h|X, Y)$, which infers the latent variable h with input X and output Y as input. Learning a CVAEs framework involves approximation of the true posterior distribution of h with a inference model $q_\phi(h|X, Y)$, where ϕ is network parameter set of the inference model.

The parameter sets of CVAEs (including both generator model parameters θ and inference model parameters ϕ) can be estimated in stochastic variational Bayes (SGVB) [16] framework by maximizing the expected variational lower bound (ELBO) as:

$$L(\theta, \phi; X) = \mathbb{E}_{q_\phi(h|X, Y)}[\log(p_\theta(Y|X, h))] - D_{KL}(q_\phi(h|X, Y) || p_\theta(h|X)), \quad (9)$$

where the first term is the expected log-likelihood and the second term measures the information lost using $q_\phi(h|X, Y)$ to approximate the true posterior distribution of latent variable h .

Following Eq. 9, we designed a CVAE based saliency detection model as shown in Fig. 4, where we add an extra encoder $q_\phi(h|X, Y)$ to the latent variable model. The encoder is composed of five convolutional layers and two fully connected layers, as shown in Table 3, where each of the fully connected layers (the last two rows in Table 3) maps the concatenation of X and Y to low dimensional vectors, including mean μ and standard deviation σ . The latent variable h is then obtained with the reparameterization trick as $h = \mu + \sigma \odot \epsilon$, where $\epsilon \in \mathcal{N}(0, I_d)$.

CGANs based Saliency Detection: Similar to the CVAE based model, two different modules (a generator and a discriminator) play the minimax game in CGANs as shown below:

$$\min_G \max_D V(D, G) = E_{(X, Y) \in p_{data}(X, Y)}[\log D(Y|X)] + E_{h \in q(h)}[\log(1 - D(G(X, h)))], \quad (10)$$

where G and D are the generator model and discriminator model respectively, $p_{data}(X, Y)$ is the joint distribution

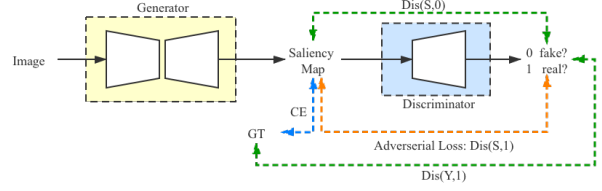


Figure 5: Network structure for training a CGAN based saliency prediction network.

Table 4: Network structure of discriminator in CGAN based saliency prediction framework.

Input Channel	Output Channel	kernel size	Stride	Padding
1	64	4	2	1
64	128	4	2	1
128	256	4	2	1
256	512	4	2	1
512	1	3	1	1

of training data, $q(h)$ is the prior distribution of the latent variable h , which is usually defined as $q(h) = \mathcal{N}(0, I_d)$. We use the same latent variable model as a generator of CGANs based saliency prediction, where the adversarial loss $Dis(S, 1)$ is cross-entropy loss, which measures the confidence of the discriminator to predict the saliency map S as real ground truth. We design a fully convolutional discriminator as [12], to distinguish per-pixel real or fake of the prediction and ground truth. Details of the discriminator network are shown in Table 4. Our CGAN based saliency detection network is shown in Fig. 5.

Generative Model Comparison: For the CVAE based framework, designing the approximate posterior network $q_\phi(h|X, Y)$ takes effort, and the imbalanced inference model may lead to the posterior collapse problem as discussed in [10], where the latent variable is independent of the prediction. For the CGAN based model, according to our experience, the training is not stable. Further, it cannot infer the latent variable h , which makes the model not explanatory. Compared with CVAEs and CGANs based models, the proposed solution is stable, and we can infer the latent variable h without an extra encoder as shown in Eq. 6 of the main paper. Further, as we directly sample from the “truth” posterior distribution via Langevin dynamics based MCMC instead of the approximated distribution, we have no posterior collapse problem.

6.6. Discussion

Performance measure for stochastic models: In this paper, we use the expectation of the learned model for a deterministic prediction to validate the method. As existing

saliency datasets do not have diverse ground truth, we can not evaluate our stochastic model at a distribution level. A possible direction is to design an image-context related saliency metric based on the assumption that image with simple context should have less diverse predictions, and vice versa. In this way, quality of stochastic model predictions can be evaluated based on both the provided single version ground truth and the input image.

The contribution of LVM for saliency detection: Firstly, compared to traditional deterministic methods, LVM has a latent variable that can handle missing data (*i.e.* scribble annotation scenario). Secondly, compared to other generative methods (*e.g.* VAE [17] or GAN [8]), ours not only has an LVM but also an EBM as a refinement engine. The iterative MCMC process refines the output provided by the LVM in minimizing the energy function, which is also to mimic reinforcement learning, where our LVM is a policy (non-iterative) and the energy function in EBM is a cost (or negative value) function (iterative process to minimize the cost function).

The advantage of combining LVM with EBM: We use the latent variable model (LVM) to generate initial prediction, and then refine it with an energy-based model (EBM). The advantage of combining LVM and EBM mainly lies in two perspectives, namely the modeling perspective and the learning perspective. Firstly, based on the subjective nature of saliency, it is natural to model the saliency given an image as a conditional probabilistic distribution instead of a deterministic regression. The proposed framework with LVM+EBM forms a rigorous generative model for this purpose. Secondly, our framework (LVM+EBM) is very different from a VAE (inference net + LVM) and a GAN (classifier + LVM) because both VAE and GAN only keep the LVM for prediction, where the inference net or classifier is discarded during testing. Differently, our system still has an EBM to further revise the prediction of the LVM, which has been proven effective with our extensive experiments.

The generative model and the scribble annotation: One of the most important power of generative models is learning from incomplete annotations. Either LVM or EBM can learn from incomplete training data. We can infer the missing observation in the latent space by computing the latent vector based on the partial annotation, and map the inferred vector back to the data space to recover the invisible part.

7. Conclusion

In this paper, we propose a generative saliency prediction model based on the conditional generative cooperative network, where a latent variable model and an energy-based model are jointly trained in a cooperative learning scheme. The latent variable model serves as a coarse saliency predictor that provides a fast initial prediction, which is then refined by Langevin revision of the energy-based model.

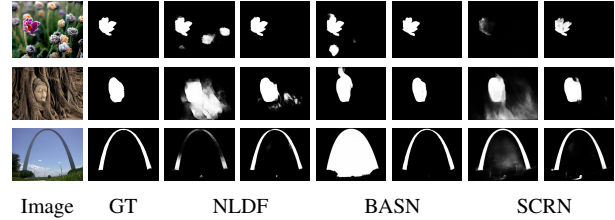


Figure 6: Visual comparison of without (“NLDF”) and with (“NLDF_R”) EBM as refinement module.

Moreover, we introduce a cooperative learning while recovering strategy and extend our model to weakly supervised saliency detection. Further, we find that the learned energy function can serve as a refinement module as post-processing technique. Extensive results illustrate effectiveness of the proposed framework.

References

- [1] Liang-Chieh Chen, George Papandreou, Iasonas Kokkinos, Kevin Murphy, and Alan L Yuille. Deeplab: Semantic image segmentation with deep convolutional nets, atrous convolution, and fully connected crfs. *IEEE Trans. Pattern Anal. Mach. Intell.*, 40(4):834–848, 2017. 5, 6, 8
- [2] Ming-Ming Cheng, Niloy J Mitra, Xiaolei Huang, and Shi-Min Hu. Salientshape: group saliency in image collections. *The Visual Computer*, 30(4):443–453, 2014. 6, 7, 8
- [3] Deng-Ping Fan, Ming-Ming Cheng, Jiang-Jiang Liu, Shang-Hua Gao, Qibin Hou, and Ali Borji. Salient objects in clutter: Bringing salient object detection to the foreground. In *Proc. Eur. Conf. Comp. Vis.* Springer, 2018. 6, 7, 8
- [4] Deng-Ping Fan, Ming-Ming Cheng, Yun Liu, Tao Li, and Ali Borji. Structure-measure: A new way to evaluate foreground maps. In *Proc. IEEE Int. Conf. Comp. Vis.*, pages 4548–4557, 2017. 6
- [5] Deng-Ping Fan, Cheng Gong, Yang Cao, Bo Ren, Ming-Ming Cheng, and Ali Borji. Enhanced-alignment Measure for Binary Foreground Map Evaluation. In *Proc. IEEE Int. Joint Conf. Artificial Intell.*, pages 698–704, 2018. 6
- [6] Mengyang Feng, Huchuan Lu, and Errui Ding. Attentive feedback network for boundary-aware salient object detection. In *Proc. IEEE Conf. Comp. Vis. Patt. Recogn.*, pages 1623–1632, 2019. 6, 7
- [7] Ruiqi Gao, Yang Lu, Junpei Zhou, Song Zhu, and Yingnian Wu. Learning generative convnets via multi-grid modeling and sampling. In *Proc. IEEE Conf. Comp. Vis. Patt. Recogn.*, pages 9155–9164, 2018. 1, 2
- [8] Ian Goodfellow, Jean Pouget-Abadie, Mehdi Mirza, Bing Xu, David Warde-Farley, Sherjil Ozair, Aaron Courville, and Yoshua Bengio. Generative adversarial nets. In *Proc. Adv. Neural Inf. Process. Syst.*, pages 2672–2680, 2014. 1, 10
- [9] Tian Han, Yang Lu, Song Zhu, and Yingnian Wu. Alternating back-propagation for generator network. In *Proc. AAAI Conf. Artificial Intelligence*, 02 2017. 8

- [10] Junxian He, Daniel Spokoyny, Graham Neubig, and Taylor Berg-Kirkpatrick. Lagging inference networks and posterior collapse in variational autoencoders. In *Proc. Int. Conf. Learning Representations*, 2019. 6, 9
- [11] K. He, X. Zhang, S. Ren, and J. Sun. Deep residual learning for image recognition. In *Proc. IEEE Conf. Comp. Vis. Patt. Recogn.*, pages 770–778, 2016. 5
- [12] Wei-Chih Hung, Yi-Hsuan Tsai, Yan-Ting Liou, Yen-Yu Lin, and Ming-Hsuan Yang. Adversarial learning for semi-supervised semantic segmentation. In *Proc. Brit. Mach. Vis. Conf.*, 2018. 3, 9
- [13] Phillip Isola, Jun-Yan Zhu, Tinghui Zhou, and Alexei A Efros. Image-to-image translation with conditional adversarial networks. In *Proceedings of the IEEE conference on computer vision and pattern recognition*, pages 1125–1134, 2017. 1
- [14] Laurent Itti, Christof Koch, and Ernst Niebur. A model of saliency-based visual attention for rapid scene analysis. *IEEE Trans. Pattern Anal. Mach. Intell.*, 20:1254 – 1259, 12 1998. 1
- [15] Danilo Jimenez Rezende, Shakir Mohamed, and Daan Wierstra. Stochastic backpropagation and approximate inference in deep generative models. In *Proc. Int. Conf. Mach. Learn.*, 2014. 2
- [16] Diederik Kingma and Max Welling. Auto-encoding variational bayes. In *Proc. Int. Conf. Learning Representations*, 2014. 2, 9
- [17] Diederik P Kingma and Max Welling. Auto-encoding variational bayes. In *Proc. Int. Conf. Learning Representations*, 2013. 2, 10
- [18] P. Knöbelreiter, C. Reinbacher, A. Shekhovtsov, and T. Pock. End-to-end training of hybrid cnn-crf models for stereo. In *Proc. IEEE Conf. Comp. Vis. Patt. Recogn.*, pages 1456–1465, 2017. 8
- [19] Simon AA Kohl, Bernardino Romera-Paredes, Clemens Meyer, Jeffrey De Fauw, Joseph R Ledsam, Klaus H Maier-Hein, SM Eslami, Danilo Jimenez Rezende, and Olaf Ronneberger. A probabilistic u-net for segmentation of ambiguous images. *Proc. Adv. Neural Inf. Process. Syst.*, 2018. 3
- [20] Hsin-Ying Lee, Hung-Yu Tseng, Qi Mao, Jia-Bin Huang, Yu-Ding Lu, Maneesh Singh, and Ming-Hsuan Yang. Dri++: Diverse image-to-image translation via disentangled representations. *Int. J. Comp. Vis.*, 128(10):2402–2417, 2020. 1
- [21] Guanbin Li, Yuan Xie, and Liang Lin. Weakly supervised salient object detection using image labels. In *Proc. AAAI Conf. Artificial Intelligence*, 2018. 2
- [22] Guanbin Li, Yuan Xie, and Liang Lin. Weakly supervised salient object detection using image labels. In *Proc. AAAI Conf. Artificial Intelligence*, 2018. 2
- [23] Guanbin Li and Yizhou Yu. Visual saliency based on multiscale deep features. In *Proc. IEEE Conf. Comp. Vis. Patt. Recogn.*, pages 5455–5463, 2015. 6, 7, 8
- [24] Jiang-Jiang Liu, Qibin Hou, Ming-Ming Cheng, Jiashi Feng, and Jianmin Jiang. A simple pooling-based design for real-time salient object detection. In *Proc. IEEE Conf. Comp. Vis. Patt. Recogn.*, 2019. 1, 2, 6, 7, 8
- [25] Nian Liu, Junwei Han, and Ming-Hsuan Yang. Picanet: Learning pixel-wise contextual attention for saliency detection. In *Proc. IEEE Conf. Comp. Vis. Patt. Recogn.*, pages 3089–3098, 2018. 2, 6, 7
- [26] Pauline Luc, Camille Couprie, Soumith Chintala, and Jakob Verbeek. Semantic segmentation using adversarial networks. In *NIPS Workshop on Adversarial Training*, 2016. 3
- [27] Zhiming Luo, Akshaya Mishra, Andrew Achkar, Justin Eichel, Shaozi Li, and Pierre-Marc Jodoin. Non-local deep features for salient object detection. In *Proc. IEEE Conf. Comp. Vis. Patt. Recogn.*, pages 6609–6617, 2017. 2, 6, 7, 8
- [28] Mehdi Mirza and Simon Osindero. Conditional generative adversarial nets. *CoRR*, abs/1411.1784, 2014. 3, 6, 8
- [29] Radford Neal. Mcmc using hamiltonian dynamics. *Handbook of Markov Chain Monte Carlo*, 06 2012. 3
- [30] Duc Tam Nguyen, Maximilian Dax, Chaithanya Kumar Mummadi, Thi-Phuong-Nhung Ngo, Thi Hoai Phuong Nguyen, Zhongyu Lou, and Thomas Brox. Deepusps: Deep robust unsupervised saliency prediction with self-supervision. In *Proc. Adv. Neural Inf. Process. Syst.*, 2019. 2
- [31] Erik Nijkamp, Mitch Hill, Song-Chun Zhu, and Ying Nian Wu. Learning non-convergent non-persistent short-run mcmc toward energy-based model. *Proc. Adv. Neural Inf. Process. Syst.*, 2019. 1, 2
- [32] Juntong Pan, Cristian Canton, Kevin McGuinness, Noel E. O'Connor, Jordi Torres, Elisa Sayrol, and Xavier and Giro-i Nieto. Salgan: Visual saliency prediction with generative adversarial networks. In *Proc. IEEE Conf. Comp. Vis. Patt. Recogn. Workshops*, 2017. 3
- [33] Xuebin Qin, Zichen Zhang, Chenyang Huang, Chao Gao, Masood Dehghan, and Martin Jagersand. Basnet: Boundary-aware salient object detection. In *Proc. IEEE Conf. Comp. Vis. Patt. Recogn.*, pages 7479–7489, 2019. 1, 2, 5, 6, 7, 8
- [34] Kihyuk Sohn, Honglak Lee, and Xinchen Yan. Learning structured output representation using deep conditional generative models. In *Proc. Adv. Neural Inf. Process. Syst.*, pages 3483–3491, 2015. 3, 8
- [35] Kihyuk Sohn, Honglak Lee, and Xinchen Yan. Learning structured output representation using deep conditional generative models. In *Proc. Adv. Neural Inf. Process. Syst.*, pages 3483–3491, 2015. 6, 8
- [36] N. Souly, C. Spampinato, and M. Shah. Semi supervised semantic segmentation using generative adversarial network. In *Proc. IEEE Int. Conf. Comp. Vis.*, pages 5689–5697, 2017. 3
- [37] Lijun Wang, Huchuan Lu, Yifan Wang, Mengyang Feng, Dong Wang, Baocai Yin, and Xiang Ruan. Learning to detect salient objects with image-level supervision. In *Proc. IEEE Conf. Comp. Vis. Patt. Recogn.*, pages 136–145, 2017. 2, 6, 7, 8
- [38] Tiantian Wang, Lihe Zhang, Shuo Wang, Huchuan Lu, Gang Yang, Xiang Ruan, and Ali Borji. Detect globally, refine locally: A novel approach to saliency detection. In *Proc. IEEE Conf. Comp. Vis. Patt. Recogn.*, pages 3127–3135, 2018. 2, 6, 7
- [39] Wenguan Wang, Jianbing Shen, Ming-Ming Cheng, and Ling Shao. An iterative and cooperative top-down and

- bottom-up inference network for salient object detection. In *Proc. IEEE Conf. Comp. Vis. Patt. Recogn.*, 2019. 1, 2
- [40] W. Wang, S. Zhao, J. Shen, S. C. H. Hoi, and A. Borji. Salient object detection with pyramid attention and salient edges. In *Proc. IEEE Conf. Comp. Vis. Patt. Recogn.*, pages 1448–1457, 2019. 2
- [41] Yang Wang, Yi Yang, Zhenheng Yang, Liang Zhao, Peng Wang, and Wei Xu. Occlusion aware unsupervised learning of optical flow. In *Proc. IEEE Conf. Comp. Vis. Patt. Recogn.*, pages 4884–4893, 2018. 6
- [42] Jun Wei, Shuhui Wang, and Qingming Huang. F3net: Fusion, feedback and focus for salient object detection. In *Proc. AAAI Conf. Artificial Intelligence*, 2020. 1, 2, 5, 6, 7
- [43] Jun Wei, Shuhui Wang, Zhe Wu, Chi Su, Qingming Huang, and Qi Tian. Label decoupling framework for salient object detection. In *Proc. IEEE Conf. Comp. Vis. Patt. Recogn.*, pages 13025–13034, 2020. 1, 2, 6, 7
- [44] Runmin Wu, Mengyang Feng, Wenlong Guan, Dong Wang, Huchuan Lu, and Errui Ding. A mutual learning method for salient object detection with intertwined multi-supervision. In *Proc. IEEE Conf. Comp. Vis. Patt. Recogn.*, pages 8150–8159, 2019. 6, 7
- [45] Zhe Wu, Li Su, and Qingming Huang. Cascaded partial decoder for fast and accurate salient object detection. In *Proc. IEEE Conf. Comp. Vis. Patt. Recogn.*, pages 3907–3916, 2019. 1, 2, 5
- [46] Zhe Wu, Li Su, and Qingming Huang. Stacked cross refinement network for edge-aware salient object detection. In *Proc. IEEE Int. Conf. Comp. Vis.*, 2019. 1, 2, 5, 6, 7, 8
- [47] Jianwen Xie, Yang Lu, Ruiqi Gao, Song-Chun Zhu, and Ying Nian Wu. Cooperative training of descriptor and generator networks. *IEEE Trans. Pattern Anal. Mach. Intell.*, 2018. 1, 2
- [48] Jianwen Xie, Yang Lu, Song-Chun Zhu, and Yingnian Wu. A theory of generative convnet. In *Proc. Int. Conf. Mach. Learn.*, volume 48, pages 2635–2644, 2016. 1, 2
- [49] Jianwen Xie, Yifei Xu, Zilong Zheng, Song-Chun Zhu, and Ying Nian Wu. Generative pointnet: energy-based learning on unordered point sets for 3d generation, reconstruction and classification. In *Proc. IEEE Conf. Comp. Vis. Patt. Recogn.*, 2021. 2
- [50] Jianwen Xie, Zilong Zheng, Ruiqi Gao, W. Wang, S. Zhu, and Y. Wu. Generative voxelnet: learning energy-based models for 3d shape synthesis and analysis. *IEEE Trans. Pattern Anal. Mach. Intell.*, 2020. 2
- [51] Jianwen Xie, Zilong Zheng, Ruiqi Gao, Wenguan Wang, Song-Chun Zhu, and Ying Nian Wu. Learning descriptor networks for 3d shape synthesis and analysis. In *Proc. IEEE Conf. Comp. Vis. Patt. Recogn.*, pages 8629–8638, 2018. 2
- [52] Jianwen Xie, Zilong Zheng, and Ping Li. Learning energy-based model with variational auto-encoder as amortized sampler. In *Proc. AAAI Conf. Artificial Intelligence*, 2021. 2
- [53] Jianwen Xie, Song-Chun Zhu, and Ying Nian Wu. Synthesizing dynamic patterns by spatial-temporal generative convnet. In *Proc. IEEE Conf. Comp. Vis. Patt. Recogn.*, pages 7093–7101, 2017. 2
- [54] Jianwen Xie, Song-Chun Zhu, and Ying Nian Wu. Learning energy-based spatial-temporal generative convnets for dynamic patterns. *IEEE Trans. Pattern Anal. Mach. Intell.*, 2019. 2
- [55] Yuan Xue, Tao Xu, Han Zhang, Rodney Long, and Xiaolei Huang. Segan: Adversarial network with multi-scale l_1 loss for medical image segmentation. *Neuroinformatics*, 16, 06 2017. 3
- [56] Qiong Yan, Li Xu, Jianping Shi, and Jiaya Jia. Hierarchical saliency detection. In *Proc. IEEE Conf. Comp. Vis. Patt. Recogn.*, pages 1155–1162, 2013. 6, 7, 8
- [57] Chuan Yang, Lihe Zhang, Huchuan Lu, Xiang Ruan, and Ming-Hsuan Yang. Saliency detection via graph-based manifold ranking. In *Proc. IEEE Conf. Comp. Vis. Patt. Recogn.*, pages 3166–3173, 2013. 6, 7, 8
- [58] Hui Yu and Xiaoxu Cai. Saliency detection by conditional generative adversarial network. In *Ninth International Conference on Graphic and Image Processing*, page 253, 04 2018. 3
- [59] D. Zhang, J. Han, and Y. Zhang. Supervision by fusion: Towards unsupervised learning of deep salient object detector. In *Proc. IEEE Int. Conf. Comp. Vis.*, pages 4068–4076, 2017. 2
- [60] Jing Zhang, Deng-Ping Fan, Yuchao Dai, Saeed Anwar, Fatemeh Sadat Saleh, Tong Zhang, and Nick Barnes. Uc-net: Uncertainty inspired rgb-d saliency detection via conditional variational autoencoders. In *Proc. IEEE Conf. Comp. Vis. Patt. Recogn.*, 2020. 2, 3
- [61] Jing Zhang, Jianwen Xie, and Nick Barnes. Learning noise-aware encoder-decoder from noisy labels by alternating back-propagation for saliency detection. In *Proc. Eur. Conf. Comp. Vis.*, 2020. 2, 6, 7
- [62] Jing Zhang, Xin Yu, Aixuan Li, Peipei Song, Bowen Liu, and Yuchao Dai. Weakly-supervised salient object detection via scribble annotations. In *Proc. IEEE Conf. Comp. Vis. Patt. Recogn.*, 2020. 2, 4, 6, 7
- [63] Jing Zhang, Tong Zhang, Yuchao Dai, Mehrtash Harandi, and Richard Hartley. Deep unsupervised saliency detection: A multiple noisy labeling perspective. In *Proc. IEEE Conf. Comp. Vis. Patt. Recogn.*, pages 9029–9038, 2018. 2
- [64] X. Zhang, X. Zhu, 3. X. Zhang, N. Zhang, P. Li, and L. Wang. Seggan: Semantic segmentation with generative adversarial network. In *2018 IEEE Fourth International Conference on Multimedia Big Data (BigMM)*, pages 1–5, 2018. 3
- [65] Yulun Zhang, Kunpeng Li, Kai Li, Lichen Wang, Bineng Zhong, and Yun Fu. Image super-resolution using very deep residual channel attention networks. In *Proc. Eur. Conf. Comp. Vis.*, 2018. 5
- [66] Huajun Zhou, Xiaohua Xie, Jian-Huang Lai, Zixuan Chen, and Lingxiao Yang. Interactive two-stream decoder for accurate and fast saliency detection. In *Proc. IEEE Conf. Comp. Vis. Patt. Recogn.*, June 2020. 6, 7
- [67] Jun-Yan Zhu, Richard Zhang, Deepak Pathak, Trevor Darrell, Alexei A Efros, Oliver Wang, and Eli Shechtman. Toward multimodal image-to-image translation. *arXiv preprint arXiv:1711.11586*, 2017. 1